Phonon instability and mechanism of superionic conduction in Li_2O

M. K. Gupta,[1] Prabhatasree Goel,[1] R. Mittal,[1,*] N. Choudhury,[1,2,3] and S. L. Chaplot[1]
[1]*Solid State Physics Division, Bhabha Atomic Research Centre, Trombay, Mumbai 400 085*
[2]*Dept. of Physics, University of Arkansas, Fayetteville, AR 72701*
[3]*Science Division, Bellevue College 3000 Landerholm Circle SE, Bellevue, WA 98007*
(Received 28 December 2011; revised manuscript received 4 April 2012; published 25 May 2012)

We report studies on the vibrational and elastic behavior of lithium oxide, Li_2O, around its superionic transition temperature. Phonon frequencies calculated using the local density approximation and generalized gradient approximation schemes of *ab initio* density functional theory are in excellent agreement with the reported experimental data. Further, volume dependence of phonon dispersion relation was calculated, which indicated softening of zone boundary transverse acoustic phonon mode along [110] at the volume corresponding to the superionic transition in Li_2O. This instability of phonon mode could be a precursor leading to the dynamic disorder of the lithium sublattice. Empirical potential model calculations were carried out to deduce the probable direction of vacancy-assisted lithium movement by constructing a supercell consisting of 12 000 atoms. The energy profile for lithium ion movement was computed at volumes corresponding to ambient and superionic regimes. The energy considerations along various symmetry directions indicated that [001] was the most favorable direction for lithium movement in the fast ion phase. This result corroborated our observation of dynamic instability in the transverse phonon mode along the (110) wave vector. Using molecular dynamics simulations, we studied the temperature variation of elastic constants, which showed a large decrease in C_{11}, consistent with known experimental observation.

DOI: 10.1103/PhysRevB.85.184304 PACS number(s): 63.20.dk, 66.30.−h, 65.40.−b

I. INTRODUCTION

Lithium oxide belongs to the class of superionics, which exhibit high ionic conductivity above 1200 K. In this case, the Li ion is the diffusing species, while oxygen ions constitute the rigid framework. Technologically, there are several applications for Li_2O, ranging from possibilities[1–3] as lightweight high-power density lithium ion batteries for heart pacemakers, mobile phones, laptop computers, etc., to high-capacity energy storage devices for next-generation clean electric vehicles, and possibly as hydrogen storage material along with Li_3N. It is also a leading contender for future fusion reactors to convert energetic neutrons to usable heat and to breed tritium necessary to sustain D-T reaction.[4] This application is attributed to its high melting point, relatively low volatility, and high Li atom density. At ambient conditions, Li_2O occurs in the antifluorite structure with space group $O^5{}_h$ $(Fm3m)$.[5–8] Oxygen ions are arranged in an fcc sublattice with lithium ions occupying the tetrahedral sites. Typically, in superionic conductors, the ionic conductivity[3] is greater than 0.01 $(\text{Ohm-cm})^{-1}$.

The novel high-temperature properties of lithium oxide and similar compounds have warranted various experimental and theoretical studies extensively.[9–33] Many theoretical techniques exist for the study of solid state, ranging from classical simulations to *ab initio* methods. Fast ion conduction makes Li_2O an ideal link between the solid and the liquid state. The main purpose of these studies has been to understand the process of fast ion conduction and the role of defects in conductivity. Earlier studies have been done to understand the migration[28,29] paths of Li ion and mechanism of diffusion. Defects and ionic diffusion in Li_2O surfaces[30] and Li_2O:B_2O_3 nanocomposites[31,32] have been studied using both first-principles methods and empirical molecular dynamics (MD) simulations. Li diffusion behavior has been studied in Li-containing oxides under fusion[34,35] reactor conditions using classical MD simulations. Such studies stem from further interest in tritium generation for future fusion reactors. There have also been studies on the high-pressure behavior,[25,26,35] change in band structure of the oxide before and after CO_2 absorption,[9] and its effect on bulk properties. Elastic behavior of the oxide with increasing pressure[34] has also been reported.

Understanding the microscopic changes at transition temperature is useful to predict new features at extreme thermodynamic conditions. Fluorites like CaF_2, BaF_2, $SrCl_2$, PbF_2, etc., show type II superionic transition. They attain high levels of ionic conductivity following a gradual and continuous disordering process within the same phase. Defect disorder (Frenkel) in the anionic sublattice is considered to be a general cause of the diffusion seen in these compounds. This is characterized by a large decrease in the elastic constant[32,33] C_{11} and a specific heat anomaly (a Schottky hump) at the transition temperature T_c. Accordingly, Li_2O shows a sudden decrease in the value of the C_{11} elastic constant at the transition temperature $T_c \sim 1200$ K (the melting point of Li_2O is 1705 K), although there does not seem to be any drastic change in the specific heat. The diffusion coefficient of lithium at this transition becomes comparable to that of liquids.[36,37]

Our earlier work[2,3] looked at the probable interstitial regions where lithium might reside while diffusing in such a way that the local structure remains largely unperturbed. Extending our earlier work with this oxide using LD and MD, we then tried to determine the probable directions of the diffusion of the lithium ions and the role of phonon and elastic instabilities. At the outset, we performed *ab initio* phonon calculations and carried out a comparative analysis with potential model calculations. Next, we tried to look at the behavior of phonon modes along symmetry directions at volumes corresponding to the superionic regime using both *ab initio* and potential model calculations. The decrease in the

elastic constants with increasing temperature was studied using potential model calculations. Superionic fluorites were found to exhibit rapid decrease in elastic constants, particularly C_{11}, and a specific heat anomaly around the transition temperature, but Li_2O did not exhibit any specific heat anomaly as observed experimentally, which is in agreement with our earlier computations. Finally, we tried to figure out the easy direction of movement of the Li ion, which is crucial in understanding the diffusion mechanism in a given system. In our earlier studies, we had inferred that Li moves from one tetrahedral site to another. In this paper, we tried to deduce the most probable direction of movement by studying the energy profile for Li movement along various high-symmetry directions. This does not rule out lithium's diffusion in other directions, but simply indicates one of the easy directions of diffusion. The study of the high-temperature behavior and their implications could play a pivotal role in understanding and improving the myriad technological applications of this immensely useful oxide.

II. COMPUTATIONAL DETAILS

The lattice dynamics (LD) calculations were performed using both empirical potential as well as *ab initio* methods. Empirical potential used was the same as in our earlier work.[2] Density functional theory (DFT) has been shown to describe the structural and lattice dynamic properties of material using pseudopotentials and plane-wave basis sets. In the framework of density functional perturbation theory (DFPT),[38] it is possible to calculate phonon frequencies, dielectric constants, and other properties. We used the Quantum ESPRESSO[39] package for the *ab initio* phonon calculations. Pseudopotentials generated by using the Perdew–Burke–Ernzerhof exchange correlation functional under generalized gradient approximation (PBE-GGA)[40] and the Perdew–Zunger correlation functional under local density approximation (PZ-LDA)[41] were used. We chose a 12 × 12 × 12 K mesh for self-consistent field calculations with energy cutoffs of 280 and 120 Rydberg for GGA and LDA, respectively, which were found to be sufficient for convergence on the order of millielectron volts. The K-point mesh was generated using the Monkhorst–Pack method.[42] Dynamical matrices were calculated on a 5 × 5 × 5 mesh with 10 q points in irreducible Brillouin zone. The force constants in real space were calculated using these dynamical matrices in the Fourier interpolation scheme,[43,44] and were further used for the calculation of phonon frequencies in the entire Brillouin zone.

By minimizing the total energy with respect to lattice parameter, we obtained the equilibrium lattice constant. The equilibrium lattice constants came out to be 4.57 and 4.45 Å for GGA and LDA approximations, respectively, at 0 K and ambient pressure, while the experimental lattice parameter[32] was 4.60 Å at 300 K. The LDA exchange correlation functional underestimated the lattice constant by 2–3%. The difference between the calculated and experimental values was ∼3%, which is acceptable under LDA. The phonon calculation was done under the constraint of the crystal acoustic sum rule. The slopes of the acoustic branches along (100) and (110) were used for the calculation of elastic constants and bulk modulus.

In our earlier MD[2] simulations, we found that a supercell consisting of 768 atoms was sufficient to obtain reliable values of diffusion coefficient. In this paper, the temperature variation of the elastic properties (in the NPT ensemble) was calculated using the MD technique. The interatomic potential was the same as used in our earlier work.[2] We calculated acoustic phonon wave velocities from the simulation of the dynamic structure factors for long wavelength acoustic phonons in several propagation directions. These calculations were carried out using a supercell ($8\mathbf{a} \times 8\mathbf{b} \times 8\mathbf{c}$) consisting of 6144 atoms with periodic boundary conditions. Such a large supercell allowed for the precise calculation of low-energy acoustic phonons of large wavelengths. The structure factor is related to the time correlation function $F(Q,t)$ of the density operator, which is given as

$$S(\vec{Q},\omega) = \int_{-\infty}^{+\infty} e^{i\omega t} F(\vec{Q},t)dt,$$

where,

$$F(\vec{Q},t) = \frac{1}{N}\langle \rho_{\vec{Q}}(t)\rho_{-\vec{Q}}(0)\rangle.$$

The density operator is given as

$$\rho_Q(t) = \sum_{i=1}^{N} e^{i\vec{Q}\cdot r_i(t)},$$

where $r_i(t)$ is the instantaneous position of the ith atom at time t.

For calculation of the energy profile for lithium movement, we created a supercell of 10 × 10 × 10 and created two lithium and one oxygen vacancies at random sites (Schottky defect). We moved an Li ion nearest to the Li vacant site and monitored the total energy without relaxing the structure. For this calculation, we used the empirical potential model.

III. RESULTS AND DISCUSSION

A. Phonon dispersion relation

Ab initio phonon calculations were carried out with both the LDA and GGA schemes. However, qualitatively, we did not get any substantial improvement using GGA. The computed values of Born effective charges for Li and O were 0.9 and

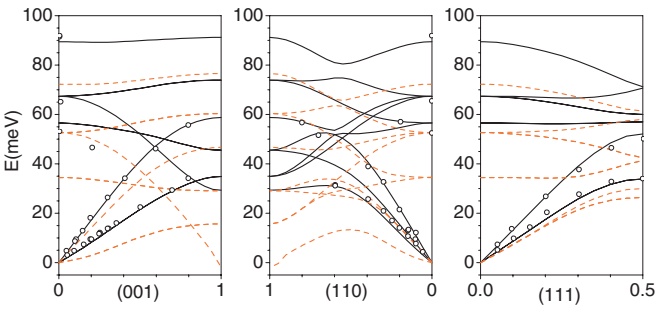

FIG. 1. (Color online) Phonon dispersion from first principles density functional theory under generalized gradient approximation (GGA-DFT). The solid and dashed lines correspond to calculations performed at $a = 4.57$ Å and $a = 4.88$ Å, respectively. The open symbols correspond to reported experimental[32] data. The lowest acoustic branch along (001) and (110) both become imaginary around the fast ion transition region.

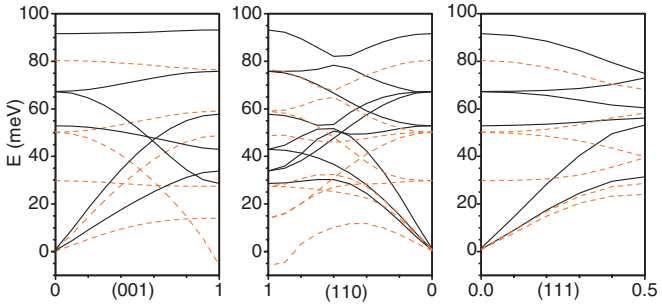

FIG. 2. (Color online) Phonon dispersion using interatomic potential in the quasiharmonic approximation. The calculations were carried out corresponding to lattice parameters at 4.60 and 4.90 Å. These values of lattice parameters were obtained from MD simulations. Phonon energies shown below $E = 0$ have imaginary values indicating unstable modes.

-1.8, respectively, while the dielectric constant was 2.90. These are in agreement with previously reported[45,46] values. Here we showed (Fig. 1) calculated phonon dispersion relation at relaxed lattice parameter $a = 4.57$ Å (at 0 K) in the GGA scheme. The phonon dispersion relation was plotted after including the longitudinal optic-transverse optic (LO-TO) splitting of the modes. The results are in good agreement with the potential model phonon dispersion calculations and reported experimental data. The compound exhibits superionic transition in the vicinity of 1200 K. Hence, we performed phonon calculations at various unit cell parameters corresponding to the superionic regime. The phonon dispersion using the potential model at lattice parameters corresponding to ambient ($a = 4.60$ Å) and superionic ($a = 4.90$ Å) regimes are shown in Fig. 2. The results obtained from the potential model are fully consistent with *ab initio* results and, therefore, the empirical potentials can be treated as first-principles-derived potentials. As expected, the phonon frequencies along all three directions were found to soften with increase of volume. The softening was found to be small for all the modes except for the lowest transverse acoustic (TA) branch along [110] at the zone boundary.

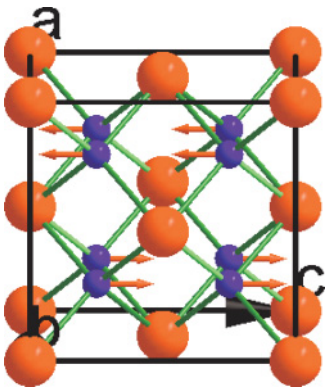

FIG. 3. (Color online) Motion of individual atoms for the zone boundary TA mode along the [110] direction at lattice parameter corresponding to $a = 4.88$ Å. The lengths of arrows are related to the displacements of the atoms. The absence of an arrow on an atom indicates that the atom is at rest; **b** axis is perpendicular to the plane. Key: O = red (dark gray) spheres, Li = blue (medium gray) spheres.

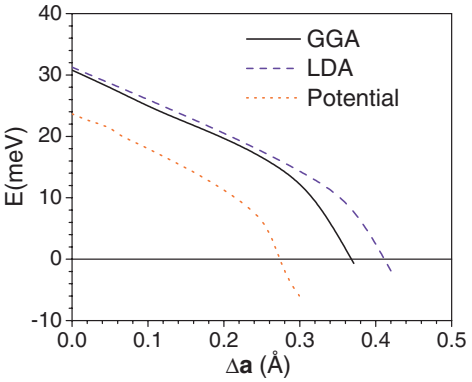

FIG. 4. (Color online) Softening of zone boundary TA phonon along [110]. $\Delta\mathbf{a}$ corresponds to the difference in lattice parameter from equilibrium. The equilibrium value of lattice parameter a in GGA, LDA, and potential model calculations are 4.57, 4.45, and 4.60 Å, respectively.

The eigenvector of the TA mode was plotted (Fig. 3) corresponding to the unit cell parameter of $a = 4.88$ Å. We found that lithium atoms in the alternate layers moved opposite to each other along [001] while oxygen atoms were at rest. The easy direction for lithium movement was along [001] (as discussed below). Hence, increasing the temperature could lead to migration of lithium ions from one site to another vacant site along the [001] direction, which can easily be visualized from Fig. 3. Figure 4 gives the change in the transverse acoustic frequency with increasing lattice parameter, as calculated from LDA and GGA schemes of *ab initio* DFT and potential model calculations. The lowest TA mode along [110] at the zone boundary was found to soften sharply at volume in the superionic regime. At the superionic transition, some of the lithium ions might just have had sufficient energy to move from their ideal positions and start diffusing. It is possible that the softening of these modes might be the precursor to the process of diffusion. Fracchia *et al.*[14] have also reported softening of the zone boundary mode along [001] in Li_2O.

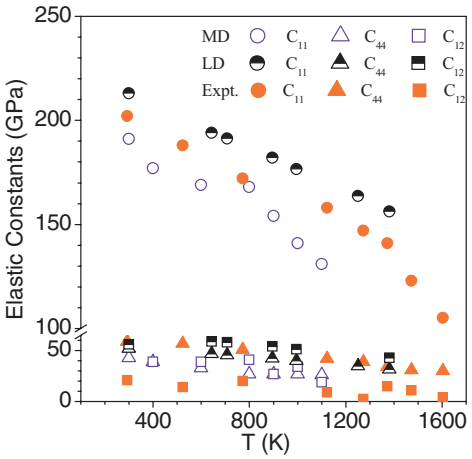

FIG. 5. (Color online) Softening of elastic constants with increasing temperature compared with reported experimental[32] results. The open, half-filled symbols correspond to the calculated values using MD and LD formalism, while solid symbols denote the reported experimental results.

TABLE I. Comparison of elastic and structural data obtained using an *ab intio* approach with available experimental results (Refs. 31 and 32) and empirical potential model calculations (Ref. 2).

Parameters	Experiment	*Ab initio* (LDA/GGA)	Potential model (Ref. 2)
Lattice constant (Å)	4.606	4.45/4.57	4.61
C_{11} (GPa)	202	234/191	213
C_{44} (GPa)	59	72/40	52
C_{12} (GPa)	21.5	31.5/45	56
B (GPa)	82	99/94	103

B. Temperature variation of elastic constants

The elastic constants obtained using the first-principles approach were compared with those obtained from potential model and reported experimental results[32,33] in Table I. Bulk modulus was calculated using the relation $B = (C_{11} + 2C_{12})/3$, where C_{11} and C_{12} are the elastic constants. The calculated elastic constants C_{11}, C_{12}, C_{44}, and bulk modulus B using the *ab initio* method at 0 K are in good agreement with reported experimental data at 300 K and our previous[2] LD calculations.

The MD technique was used to calculate the effect of temperature on the elastic properties. We found that increasing temperature resulted in significant change in the acoustic phonon frequencies, which in turn brought a change in the elastic properties. The calculations were found to be in good comparison (Fig. 5) with the reported experimental data.[32] Here, C_{11} showed maximum softening, which is one of the characteristic features of a superionic compound. The change in C_{12} was marginal, while C_{44} remained almost constant with temperature increase. The gradual change in C_{44} and C_{12} with increasing temperature was brought out better in the MD simulation and is in good agreement with experimental findings. With increasing temperature, most of the phonon modes shifted towards lower energy. The details of dependence of elastic constants on temperature could play a pivotal role in understanding the role and uses of lithium oxide as blanket material for tritium production in fusion reactors.

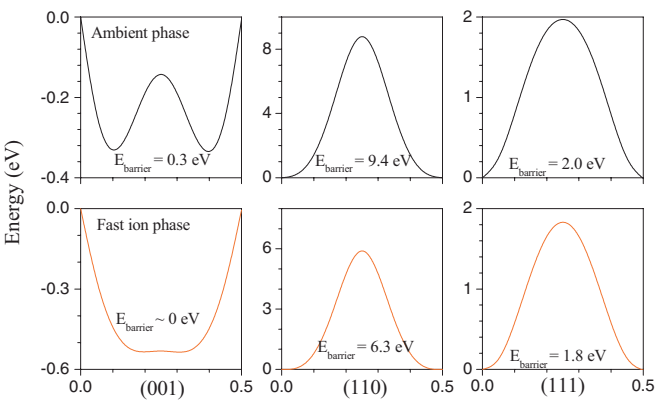

FIG. 6. (Color online) Energy profile for lithium ion movement along high-symmetry directions. Calculations were carried out using a 10 × 10 × 10 supercell corresponding to lattice parameter values of 4.606 and 4.88 Å.

C. Energy profile for Li movement

The movement of atoms in a material depends on the interatomic bonding, temperature, microstructure, size, and type of atoms moving. The energy profile for lithium movement was calculated by creating a vacancy and moving a lithium atom from its initial lattice site towards the vacant lattice site along a given high-symmetry direction, namely [001], [110], and [111] directions in a 10 × 10 × 10 supercell, and monitoring the change in the total crystal potential. The charge neutrality of the supercell was maintained in the complete process. This enabled us to identify the easy direction for Li motion towards vacancy at different temperatures. The profiles of the energy changes are shown in Fig. 6. The calculated energies for movement of Li atom along [001], [110], and [111] directions were 0.3(0.0), 9.4(6.3), and 2.0(1.8) eV, respectively, at unit cell volumes corresponding to 4.60 and 4.88 Å. It can be seen that the most favorable direction for lithium movement was along the [001] direction. With increase in temperature, the increased availability of defects and vacancies could lead to a simultaneous movement of several lithium ions towards their nearest vacant site. This cooperative phenomenon could lead to a macroscopic effect of diffusion, which is observed in Li_2O above superionic temperature, but this does not rule out lithium's motion along a combination of other directions.

IV. CONCLUSIONS

A combination of classical and first-principles studies were used to successfully explain the behavior of lithium oxide at the onset of superionic transition. Phonon dispersion along symmetry directions from *ab initio* calculations is in good agreement with reported experimental data. We found that, around the fast ion transition temperature, the zone boundary TA phonon mode along [110] became unstable. This softening of the phonon could be a precursor to dynamic instability. This observation is corroborated by the eigenvector of this mode and could be one of the factors leading to diffusion of lithium ions. We also were able to simulate the decrease in elastic constants with increasing temperature, which is one of the characteristic features exhibited by these fast ion conductors. Finally, we were able to relate the phonon softening with the ease of lithium movement at an elevated temperature along [001] as against the other two high-symmetry directions considered. These studies shed more light on and can aid in improving the utilization of the oxide in its numerous technological applications.

*rmittal@barc.gov.in

[1] T. W. D. Farley, W. Hayes, S. Hull, M. T. Hutchings, and M. Vrtis, J. Phys.: Condens. Matter **3**, 4761 (1991).

[2] P. Goel, N. Choudhury, and S. L. Chaplot, Phys. Rev. B **70**, 174307 (2004).

[3] P. Goel, N. Choudhury, and S. L. Chaplot, J. Phys.: Condens. Matter **19**, 386239 (2007); Pramana-J. Phys. **63**, 409 (2004).

[4] David A. Keen, J. Phys.: Condens. Matter **14**, R819 (2002).

[5] G. L. Kalucinki, J. Nucl. Mater. **141**, 3 (1986).

[6] R. Shah, A. De Vita, H. Heine, and M. C. Payne, Phys. Rev. B **53**, 8257 (1996).

[7] R. W. G. Wyckoff, in *Crystal Structures*, 2nd ed. (John Wiley & Sons, New York, 1963).

[8] Leonid Azaroff, J. Appl. Phys. **32**, 1658 (1961); **32**, 1663 (1961).

[9] Y. Duan and D. C. Sorescu, Phys. Rev. B **79**, 014301 (2009).

[10] M. Ricco, M. Belli, M. Mazzani, D. Pontiroli, D. Quintavalle, A. Janosky, and G. Csayi, Phys. Rev. Lett. **102**, 145901 (2009).

[11] K. Kang, D. Morgan, and G. Ceder, Phys. Rev. B **79**, 014305 (2009).

[12] B. Rolling and M. D. Ingram, Phys Rev. B **56**, 13619 (1997).

[13] I. Svare, F. Borsa, D. R. Torgeson, and S. W. Martin, Phys. Rev. B **48**, 9336 (1993).

[14] R. M. Fracchia, G. d. Barrera, N. L. Allen, T. H. K. Barron, and W. C. Mackrodt, J. Phys. Chem. Solids **59**, 435 (1998).

[15] S. Adams, J. Solid State Electrochem. **14**, 1787 (2010).

[16] G. Carini, M. Cutreni, A. Fontana, G. Mariotto, and F. Rocco, Phys. Rev. B **29**, 3567 (1984).

[17] M. Mangion and G. P. Johari, Phys. Rev. B **36**, 8845 (1987).

[18] D. L. Sidebottom, P. F. Green, and R. K. Brow, Phys. Rev. B **51**, 2770 (1995).

[19] M. Porto, P. Masass, M. Meyer, A. Bunde, and W. Dieterich, Phys. Rev. B **61**, 6057 (2000).

[20] T. J. Pennycook, M. J. Beck, K. Vagra, M. Varela, S. J. Pennycook, and S. T. Pantelides, Phys. Rev. Lett. **104**, 115901 (2010).

[21] L. E. Sanchez-diaz, A. Vizcara-Rendon, and R. Juarez-Maldonado, Phys. Rev. Lett. **103**, 035701 (2009).

[22] D. L. Sidebotom, Phys. Rev. Lett. **82**, 3653(1999).

[23] B. Rolling and C. Martiny, Phys. Rev. Lett. **85**, 1274 (2000).

[24] C. Ouyuang, Siqi Shi, Zhaoxiang Wang, X. Huang, and L. Chen, Phys. Rev. B **69**, 104303 (2004).

[25] A. Lazicki, C. S. Yoo, W. J. Evans, and W. E. Pickett, Phys. Rev. B **73**, 184120 (2006).

[26] K. Kunc, I. Loa, and K. Syassen, Phys. Rev. B **77**, 094110 (2008).

[27] W. Dietrich, P. Fulde, and J. Peschel, Adv. Phys. **29**, 527 (1980).

[28] M. Hayoun, M. Meyer, and A. Denieport, Acta Mater. **53**, 2867 (2005).

[29] M. Hayoun and M. Meyer, Acta Mater. **56**, 1366 (2008).

[30] M. M. Islam and T. Bredow, J. Phys. Chem. C **113**, 672 (2009).

[31] M. M. Islam, T. Bredow, S. Indris, and P. Heitjans, Phys. Rev. Lett. **99**, 145502 (2007).

[32] S. Hull, T. W. D. Farley, W. Hayes, and M. T. Hutchings, J. Nucl. Mater. **160**, 125 (1988).

[33] T. W. D. Farley, W. Hayes, S. Hull, and R. Ward, Solid State Ionics **28–30**, 189 (1988).

[34] L. X. Fang, C. Xiang-Rong, J. Guang-Fu, and M. Chuan-Min, Chin. Phys. Lett. **23**, 925 (2006).

[35] L. Xiao-Feng, C. Xian-Rong, M. M. Chuan, and J. Guang-Fu, Solid State Commun. **13**, 197 (2006).

[36] T. Kurusawa, T. Takahashi, K. Noda, H. Takeshita, S. Nasu, and H. Watanbe, J. Nucl. Mater. **107**, 334 (1982).

[37] Takuji Oda and S. Tanaka, J. Nucl. Mater. **386**, 1087 (2009).

[38] S. Baroni, P. Giannozzi, and A. Testa, Phys. Rev. Lett. **58**, 1861 (1987).

[39] P. Giannozzi, S. Baroni, N. Bonini, M. Calandra, R. Car, C. Cavazzoni, D. Ceresoli, G. L. Chiarotti, M. Cococcioni, I. Dabo, A. D. Corso, S. de Gironcoli, S. Fabris, G. Fratesi, R. Gebauer, U. Gerstmann, C. Gougoussis, A. Kokalj, M. Lazzeri, L. Martin-Samos, N. Marzari, F. Mauri, R. Mazzarello, S. Paolini, A. Pasquarello, L. Paulatto, C. Sbraccia, S. Scandolo, G. Sclauzero, A. P. Seitsonen, A. Smogunov, P. Umari, and R. M. Wentzcovitch, J. Phys. Condens. Matter **21**, 395502 (2009).

[40] J. P. Perdew, K. Burke, and M. Ernzerhof, Phys. Rev. Lett. **77**, 3865 (1996).

[41] J. P. Perdew and A. Zunger, Phys. Rev. B **23**, 5048 (1981).

[42] H. J. Monkhorst and J. D. Pack, Phys. Rev. B **13**, 5188 (1976).

[43] X. Gonze and C. Lee, Phys. Rev. B **55**, 10355 (1997).

[44] M. M. Beg and S. M. Shapiro, Phys. Rev. B **13**, 1728 (1976).

[45] P. Sony and A. Shukla, Phys. Rev. B **77**, 075130 (2008).

[46] P. Sony and A. Shukla, Phys. Rev. B **73**, 165106 (2006).